CORROSION SCIENCE AND TECHNOLOGY, Vol.31, No.4(2002), pp.265~274

# Surface Oxide Films Affecting Metallic Corrosion

**Norio Sato**

*Corrosion Research Group, Graduate School of Engineering, Hokkaido University*
*Kita-Ku, Sapporo, Hokkaido, 060-8628 Japan*

Depending on their ionic and electronic properties, surface oxides influence metallic corrosion in aqueous solutions. The ion-selective property controls the transport of ions through the surface oxide, and the electronic property of the oxide influences the electrode potential of corroding metals. Anion-selective surface oxides accumulate corrosive anions accelerating the metallic corrosion, whereas cation-selective oxides inhibit the corrosion by removing corrosive hydrogen ions from the metal surface. The presence of n-type surface oxides lowers the corrosion potential to decrease the metallic corrosion, while p-type surface oxides raise the corrosion potential accelerating the corrosion. Photoexcitation enhances these electronic effects of semiconducting surface oxides on the corrosion.

***Keywords*** : *surface oxide films, ion-selectivity, corrosion potential, semiconducting oxides, photopotential..*

## 1. Introduction

Metallic corrosion in aqueous solutions produces a layer of corrosion precipitates on the metal surface. The interfacial layer thus produced influences of underlying metals depending on its ionic and electronic properties. The presence of a gel-like or porous precipitate layer of insoluble rusts such as hydrous metal salts or oxides causes either accelerated metallic corrosion or passivation.[1-5] Furthermore, even a compact surface oxide makes the corrosion either accelerated or decelerated depending on its coverage and electronic nature.[6),7)]

The local corrosion cell involves the transport of hydrated ions through a surface layer and the ionic concentration under the layer is determined by the ion-selective nature of the layer.[5),6),8)] Rust layers of hydrous metal oxides are either anion- or cation-selective. Huber[10)] found that a layer of aluminum oxide ($Al_2O_3$) formed on metallic aluminum is anion-selective in a potassium chloride solution and cation-selective in a sodium hydroxide solution. Suzuki et al.[11)] found that an artificially formed membrane of hydrous ferric oxide is anion-selective in a potassium chloride solution. Sakashita et al.[12-20)] found that the ion-selective property of membranes of hydrous iron oxides,[12-15)] nickel oxides[16-19)] and chromium oxides[20)] depends on the pH and hydrated ions in aqueous solutions.

The electronic property of surface oxides also influences the corrosion of underlying metals. We have suggested for metals partly covered with semiconducting oxides that metallic corrosion is acceleratedby n-type oxides and decelerated by p-type oxides.[7)]

This article discusses and summarizes the effects of the ionic and the electronic nature of surface hydroxide and oxide films on the corrosion of underlying metals.

## 2. Ionic transport through surface rust layers (ionic nature)

### 2.1 The ion-selectivity of rust layers

The ion-selective nature of porous rusts is determined by the charge fixed in the inner pores of the rusts; it is anion-selective with the positive fixed charge and cation-selective with the negative fixed charge. In general, surface rust precipitates contain the positive fixed charge in acidic solutions and the negative fixed charge in basic solutions, and they are thus anion-selective in acidic solutions and cation-selective in basic solutions.[8),9)] There is a critical pH at which a hydrous metal oxide changes its ion-selective nature, a pH which is called the point of iso-selectivity, $pH_{pis}$[8),9),15)] : in sodium chloride solutions $pH_{pis}$=10.3 for hydrous ferric oxides and $pH_{pis}$=5.8 for hydrous ferric-ferrous mixed oxides.[8),9)]

The ion-selective property of hydrous metal oxides is affected by the adsorption of multivalent ions in the inner pores.[9),14),15)] Anion-selective oxides change their fixed charge from the positive to the negative sign through the adsorption of multivalent oxoanions and hence shift the point of iso-selectivity toward acidic pH;hydrous ferric oxides are anion-selective in neutral sodium chloride solutions but turn to be cation-selective with adsorbed mul

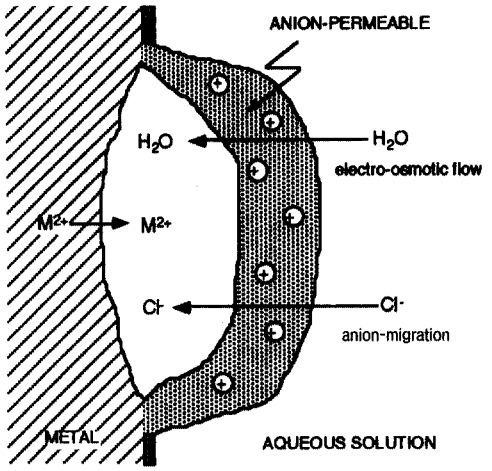


**Fig. 1.** Chloride ion condensation and acidification in an occluded solution under an anion-selective rust layer on corroding metals in aqueous chloride solutions.

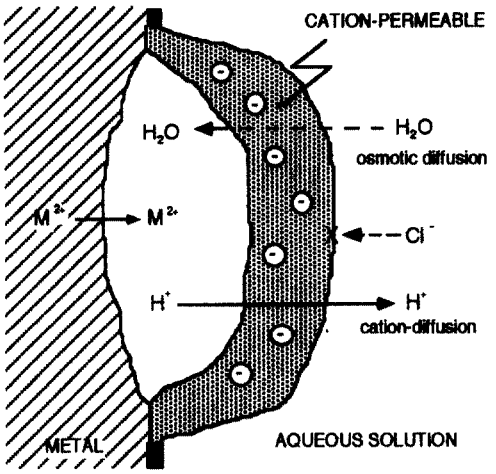


**Fig. 2.** Proton depletion and basification in an occluded solution under a cation-seletive rust layer on corroding metals in aqueous solutions.

tivalent oxoanions such as divalent molybdate anions, divalent sulphate anions and trivalent phosphate anions.[9),14),15)] Such a change in the ion-selectivity of rust layers frequently plays an important role in the corrosion of metals.

### 2.2 Anion-selective rust layers

The anodic metal corrosion under an anion-selective rust layer is followed by an anodic ion transport mainly carried by chloride ions migrating across the layer into an occluded solution as shown in Fig. 1. The chloride accumulation then reaches the level at which the rate of inward migration equals the rate of outward diffusion of chloride ions in the occluded solution. Furthermore, the anodic chloride ion migration is accompanied by the electro-osmotic flow of water molecules into the occluded solution. In the steady state the final chloride concentration is proportional to the ratio of the electro-migration rate of chloride ions to the electro-osmotic flow rate of water molecules.[21)] The transference number of water molecules in the anion- selective rust layer thereby plays a decisive role in determining the final chloride concentration in the occluded solution.

Sine the transference number of water molecules decreases with deereasing size of the inner pore in the rust,[21)] the smaller pore size and hence the less porous rust layer causes the higher chloride concentration. As the soluble metal chloride concentration increases, acidification occurs in the occluded solution, thus accelerating the metallic corrosion. In general, the anion-selective rust layer increases the corrosion of underlying metals.

### 2.3 Cation-selective rust layers

The anodic ion transport across a cation selective rust layer is mainly carried by hydrated protons migrating from the occluded solution to the bulk solution as shown in Fig. 2. No chloride ion accumulation and no acidification occur in the occluded solution as a result. The proton depletion causes the basification leading to the precipitation of metal hydroxides under a cation selective rust layer. Furthermore, the electro-osmotic flow of water molecules accompanied by the proton migration suppresses the diffusion of water molecules from the bulk solution to the level at which the dehydration of the occluded solution may occur.

Since the metal dissolution requires several water molecules for one metallic ion to hydrate, the depletion of water molecules will reduce the metallic corrosion. In general, the cation-selective rust layer prevents the corrosion of underlying metals.

### 2.4 Bipolar ion-selective rust layers

When multivalent oxoanions, such as phosphate ions and molybdate ions, are adsorbed on an anion-selective rust layer, an anodically backward bipolar layer is formed consisting of an anion-selective inner layer and a cation-selective outer layer as shown in Fig. 3. The ion transport in such a bipolar layer is prevented from occurring in the anodic direction. As the anodic polarization increases, the electric field in the neutral transition layer increases to the level at which the dissociation of water molecules makes the anodic ion transport occur as shown in Fig. 4. The rust layer is thus dehydrated to produce a compact corrosion-resistive oxide rust on the metal surface.

In general, the bipolar ion-selective rust layer inhibits the corrosion and induces the passivation of underlying metals.

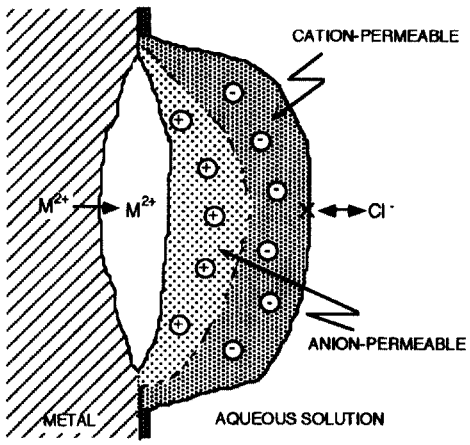


**Fig. 3.** Anodic ion transport suppressed in an anodically backward bipolar ion-selective rust layer on corroding metals in aqueous solutions.

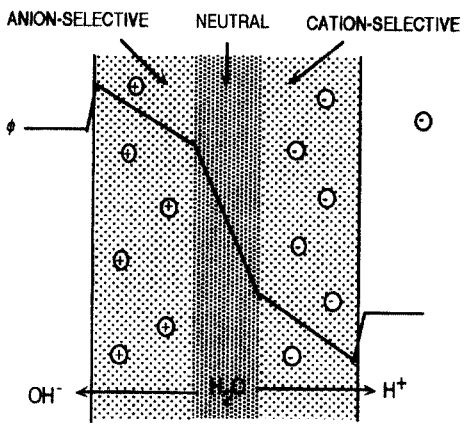


**Fig. 4.** Profile of the electrostatic potential across an anodically backward bipolar ion-selective rust layer and dehydration of the rust layer on metals.[5]

### 2.5 Non-selective layers and dehydrated layers

The ion-selective transport no longer proceeds when the ionic conecentration is much greater than the fixed charge concentration in the inner pores of the rust layer. Such a situation may be realized if the surface rust is formed with relatively large pores containing concentrated ionic solutions. In conentrated ionic solutions the usual ionic diffusion and migration prevail over the ion-selective transport in the pores.

On the other hand, if the pore size is so small that no hydrated ions may be transported through the pores, the solid-state-diffusion of ions prevails in the rust layer. Such a compact layer of surface oxides, if covering the metal surface completely without defects or cracks, brings the metal into the passive state. If a compact oxide layer covers the metal surface not completely but partly, the oxide affects the corrosion of the metal as described in the following.

## 3. Semiconducting surface oxides on metals (eectronic nature)

### 3.1 The electrode potential of oxide-covered metals

The absolute electrode potential of an oxide-covered electrode, $E_{(M/MO/H_2O/V)}$, is expressed in terms of the real potential of electrons, $a_{e(M/MO/H_2O/V)}$, the energy for an electron to transfer from the outer potential through the aqueous solution and the oxide film into the electron level (Fermi level) in the electrode metal[22] as shown in Eq. 1:

$$E_{(M/MO/H_2O/V)} = -\frac{a_{e(M/MO/H_2O/V)}}{e} = \chi_{H_2O/V} + \Delta\varnothing_{MO/H_2O} + \Delta\varnothing_{M/MO} - \frac{\mu_{e(M)}}{e} \quad (1)$$

where $\chi_{H_2O/V}$ is the surface potential of the solutions, $\Delta\varnothing_{MO/H_2O}$ is the potential gap at the $MO/H_2O$ interface, $\Delta\varnothing_{M/MO}$ is the potential gap at the M/MO interface, and $\mu_{e(M)}$ is the chemical potential of electrons in the electrode metal.

The oxide-covered metal electrodes can be classified into two types; the ionic $M/MO/H_2O$ electrodes and the electronic $M/MO/H_2O$ electrodes. The former consists of the ionic transfer processes only that occur across the M/MO and the $MO/H_2O$ interfaces, while the latter is formed when only the electronic transfer is equilibrium at the two interfaces.

### 3.2 Ionic $M/MO/H_2O$ electrodes

The ionic $M/MO/H_2O$ electrode consists of the metal ion transfer across the M/MO interface and the oxide ion transfer across the $MO/H_2O$ interface as represented by $M_M^{2+} + H_2O = MO + 2H_{aq}^+$ in Fig. 5(a). The electrode potential of this ionic electrode corresponds to the electrode potential of the metal oxide formation in aqueous solutions, $M + H_2O = MO + 2H_{aq}^+ + 2e_M$.

The profile in the electrostatic potential is shown in Fig. 5 (b), in which the activity of metal ion vacancies is assumed constant throughout the oxide layer. If a gradient in the vacancy activity exists, a potential gradient arises in the oxide layer reducing the two interfacial potentials so as to maintain the overall electrode potential constant.

### 3.3 Electronic $M/MO/H_2O$ electrodes

The electronic $M/MO/H_2O$ electrode consists of the

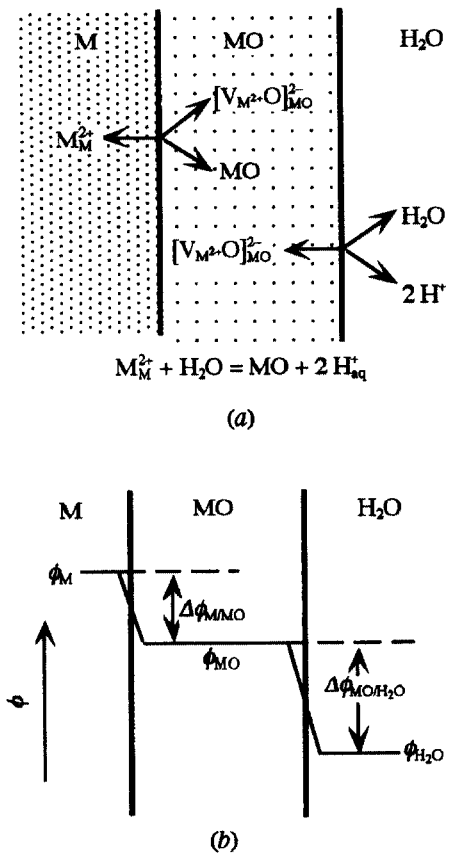


**Fig. 5.** Schemata for (a) the ion transfer and for (b) the electrostatic potential at an ionic M/MO/$H_2O$ electrode: $[\ V_{M^{2+}} + O]^{2-}_{MO}$ = the metal ion vacancy in the oxide phase.

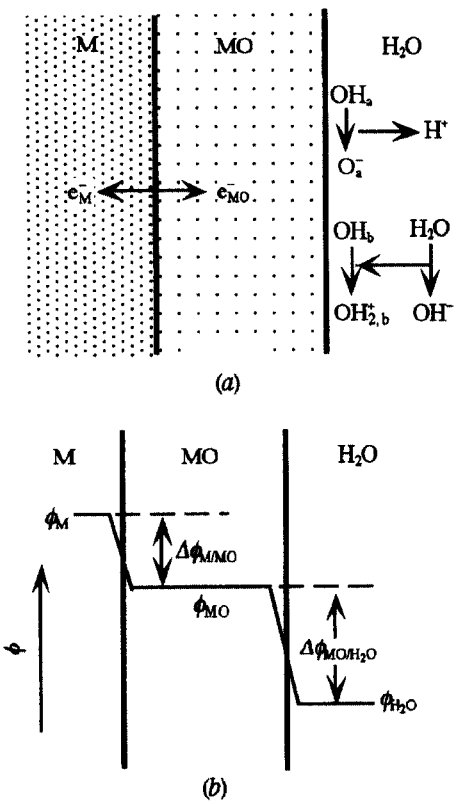


**Fig. 6.** Schemata for (a) the electron transfer combined with the interfacial acid-base dissociation and for (b) the electrostatic potential at an electronic M/MO/$H_2O$ electrode.

electron transfer across the M/MO interface and the acid-base dissociation of adsorbed hydroxyl groups at the MO/$H_2O$ interface as shown in Fig. 6(a). The electrode potential of this electronic oxide electrode is obtained as shown in Eq.2:

$$E_{(M/MO/\,H_2O/V)} = \triangle\varnothing^{O}_{H_{(MO/\,H_2O)}} + \chi_{H_2O/V} - \frac{\mu_{e(MO)}}{e} + \frac{kT}{e}\ln(a_{H^+_{aq}}) = E^{O(electron)}_{(M/MO/\,H_2O/V)} + \frac{kT}{e}\ln(a_{H^+_{aq}}) \quad (2)$$

where $E^{O(electron)}_{(M/MO/\,H_2O/V)}$ is the standard potential of the electronic oxide. The profile in electrostatic inner potential is shown in Fig. 6(b), where no space charge is assumed existing in the metal oxide layer.

Eq. 2 notes that the electrode potential of an electronic oxide is independent of the chemical potential of electrons in the electrode metal, depending though on the chemical potential of electrons in the oxide. The electrode potential thereby remains unchanged whatever electrode metals M′ are used [M′/MO/$H_2O$].

This potential is called the *flat band potential* of the oxide and represents the energy level of electrons [Fermi level] in the oxide, with which equilibrated is the Fermi level in the electrode metal.

### 3.4 Mixed electrodes of metal and metal oxide

A mixed electrode arises when a metal electrode partly covered with an oxide is brought in aqueous solutions. The oxide electrode behaves either as an electronic electrode or an ionic electrode. Only the former case is discussed as shown in Fig. 7.

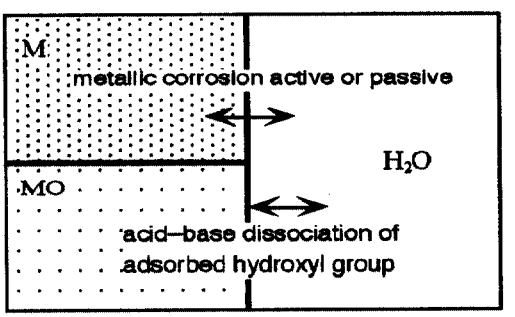


**Fig. 7.** A mixed electrode consisting of a metal oxide and a corroding metal in aqueous solutions.

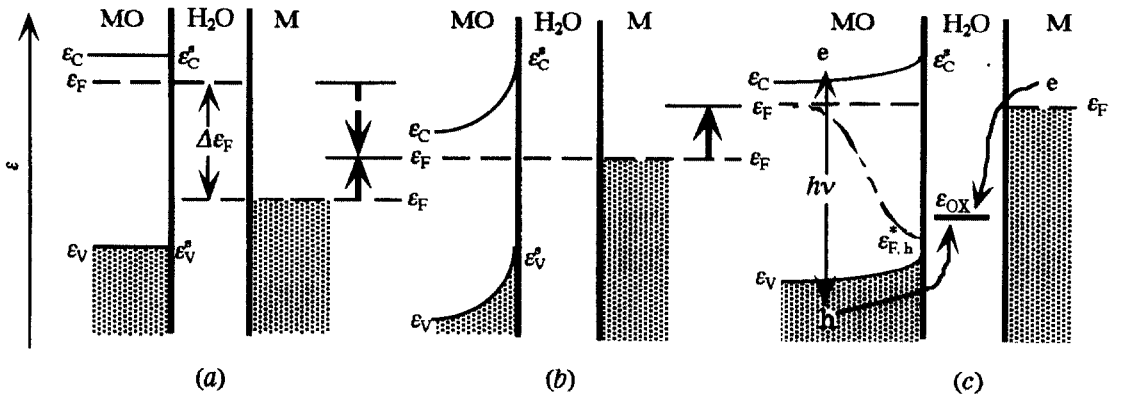


**Fig. 8.** Electronic energy levels in a metal and an n-type semiconducting oxide electrode (a) prior to, (b) posterior to electronic contact without photoexcitation, and (c) with photoexcitation: $\varepsilon_F$=Fermi level; $\varepsilon^{s}_{C}$=conduction band edge level at the MO/$H_2O$ interface; $\varepsilon^{s}_{V}$= valence band edge level at the MO/$H_2O$ interface; $\varepsilon^{*}_{F,h}$= quasi-Fermi level of interfacial holes in photoexcited oxides; $h\nu$ =photon energy; $\varepsilon_{OX}$=Fermi level of redox electrons in the oxygen reaction.

### 3.5 Semiconducting n-type metal oxide on corrodible metals

Prior to their electronic contact, an n-type oxide electrode stands at its flat band potential and a metallic electrode stands at its corrosion potential. Fig. 8(a) shows the electronic level in the two separate electrodes. The Fermi level is usually higher in n-type oxides than in common metals, $\varepsilon_{F(MO)} > \varepsilon_{F(M)}$, and the flat band potential of the oxide, $E_{fb}$ is thus more cathodic than the corrosion potential of metals, $E_{corr}$. Electronic contact equilibrates the Fermi level in the two phases, forming a space charge layer in the n-type oxide electrode and altering the interfacial potential [Helmholtz layer potential] at the metal electrode. The Fermi level of the oxide is lowered [the electrode potential of the oxide becomes more anodic] as a result, and accordingly the Fermi level of the metal is raised [the metallic corrosion potential becomes more cathodic] as shown in Fig. 8(b).

Photon illumination on semiconductor electrodes is known to produce excited electron-hole pairs reducing the space charge potential in the electrodes: the potential shift thus produced by photoexcitation is called the photopotential. With n-type oxides the photoexcitation raises the Fermi level toward the flat band level shifting the mixed electrode potential in the cathodic direction toward the flat band potential as shown in Fig. 8(c). The photoexcitation thereby shifts the potential further in the cathodic direction reducing the probability of metallic corrosion.

The metal oxides that can lower the electrode potential of contacting metals are usually n-type semiconductors, since the flat band potential is much lower in n-type semiconductors than in p-type semiconductors. Observations[23-25] have shown that metallic copper and stainless steel were prevented from corrosion when they were brought in contact with n-type titanium oxides.

The photoexcitation generates in n-type oxides concentrated holes in the space charge layer and lowers the quasi-Fermi level(effective Fermi level) of photoexcited holes[26] toward the valence band edge as shown in Fig. 8(c). With some n-type oxides such as titanium oxide the photoexcitation brings the interfacial quasi-Fermi level, $\varepsilon^{*}_{F,h}$, down to a level lower than the Fermi level of redox holes, $\varepsilon_{OX}$, in the oxygen reaction of Eq.3:

$$2H_2O + 4h_{redox} = O_2 + 4H^{+}_{aq} \qquad (3)$$

where $h_{redox}$ is the redox hole in the oxygen reaction. As the interfacial quasi-Fermi level, $\varepsilon^{*}_{F,h}$, becomes lower than redox hole level of oxygen, $\varepsilon_{OX}$, the anodic reaction of oxygen evolution is allowed to proceed on the oxide, even if the Fermi level, $\varepsilon_F$, in the bulk of the oxide electrode is much higher than the redox hole level of oxygen, $\varepsilon_{OX}$, as shown in Eq. 4:

$$2H_2O + 4h_{MO} \rightarrow O_2 + 4H^{+}_{aq} \quad \text{on the oxide part} \qquad (4)$$

This photoexcited oxygen evolution occurs on the oxide even at electrode potentials much more cathodic than the equilibrium oxygen potential, at which potentials however the cathodic reduction of oxygen(and proton if the potential is more cathodic than the hydrogen potential) proceeds on the metal surface as shown in Eq. 5:

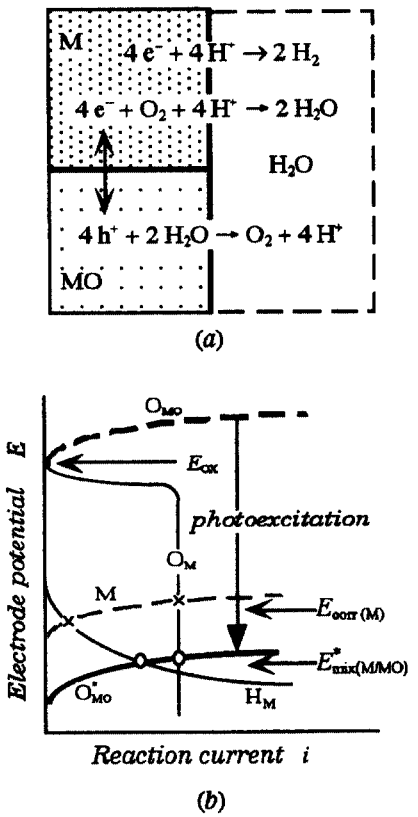


**Fig. 9.** Schemata for (a) local cell reactions and (b) their polarization curves at the M/$H_2O$ and MO/$H_2O$ interfaces on the photoexcited M-MO/$H_2O$ mixed electrode with an n-type semiconductor MO:M = anodic polarization curve of metal dissolution; $E_{OX}$ = equilibrium oxygen electrode potential;$O_M$ = cathodic polarization curve of oxygen reduction at the M/$H_2O$ interface;$H_M$ = cathodic polarization curve of proton reduction at the M/$H_2O$ interface;$E_{corr}$=corrosion potential of an isolated metal; $O^*_{MO}$=anodic polarization curve [Fermi level of electrons versus current] of the oxygen evolution at the MO/$H_2O$ interface;$O_{MO}$=anodic invisible polarization curve [interfacial quasi-Fermi level of exited holes versus current] of the oxygen evolution at the MO/$H_2O$ interface; $E_{mix}$ = mixed electrode potential of a photoexcited M-MO/$H_2O$ mixed electrode in the presence of oxygen.

$$O_2 + 4H^+_{aq} + 4e_M \rightarrow 2\,H_2O \quad \text{on the metal part} \qquad (5a)$$

$$2e_M + 2H^+_{aq} \rightarrow H_2 \quad \text{on the metal part} \qquad (5b)$$

Under photoexcitaation conditions, consequently, the cathodic oxygen reduction on the metal may be coupled with the anodic oxygen evolution on the oxide as shown in Fig. 9(a).

Fig. 9(b) schematically shows the polarization curves of anodic and cathodic reactions that will occur on the metal/n-type oxide mixed electrode under the dark and photoexcited conditions.

### 3.6 Semiconducting p-type metal oxides on corrodible metals

Fig. 10(a) shows the electronic level in two electrodes of a metal and a semiconducting p-type oxide prior to and posterior to their electronic contact;the Fermi level is usually lower in p-type oxides than in common metals, $\varepsilon_{F(MO)} < \varepsilon_{F(M)}$ and hence $E_{fb} > E_{corr}$. Electronic contact equilibrates the Fermi level in the two electrodes, forming a space charge layer in the p-type oxide electrode and altering the Helmholtz layer potential of the corroding metal electrode. Accordingly, the Fermi level of the metal is lowered[the corrosion potential becomes more anodic] as shown in Fig. 10(b), and the metallic corrosion is thus increased.

Photoexcitation produces in p-type oxide excited electrons which reduce the space charge potential, lower the Fermi level, and shift the mixed electrode potential in the anodic direction toward the flat band potential (photopotential) as shown in Fig. 7(c). The photoexcitation thereby shifts the corrosion potential further in the anodic direction, increasing further the metallic corrosion.

The photoexcited electrons raise the quasi-Fermi level toward the conduction bandedge[26] as shown in Fig. 10(c). As the interfacial quasi-Fermi level, $\varepsilon^*_{F,e}$, becomes higher than the Fermi level of redox electrons, $\varepsilon_{HY}$, of the hydrogen reaction (Eq.6), the cathodic hydrogen evolution is allowed to occur on the oxide even if the Fermi level, $\varepsilon_F$, in the bulk oxide is much lower than the Fermi level of redox electrons in the hydrogen reaction, $\varepsilon_{HY}$:

$$H_2 = 2H^+_{aq} + 2e_{redox} \qquad (6)$$

where $e_{redox}$ is the redox electron of the hydrogen reaction.

Accordingly, under photoexcitation condition the anodic metal dissolution of Eq. 7 may be coupled with the cathodic hydrogen evolution of Eq.8 on the oxide:

$$M^{2+}_M \rightarrow M^{2+}_{aq} \quad \text{on the metal part} \qquad (7)$$

$$2H^+_{aq} + 2\,e_M \rightarrow H_2 \quad \text{on the oxide part} \qquad (8)$$

The cathodic photoexcited hydrogen evolution proceeds even at electrode potentials much more anodic than the hydrogen potential.

Fig. 11(b) schematically shows the polarization curves of anodic and cathodic reactions that will occur on the metal/p-type oxide mixed electrode under the dark and photoexcited conditions.

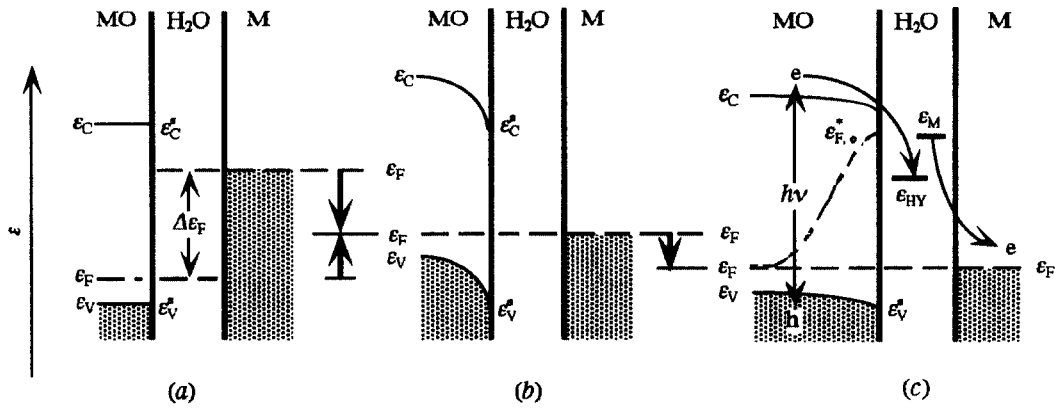


**Fig. 10.** Electronic energy levels in a metal and a p-type semiconducting metal oxide electrode (a) prior to, (b) posterior to the electronic contact without photoexcitation, and (c) with photoexitation: $\varepsilon^{*}_{F,e}$ = quasi-Fermi level of interfacial photoexcited electrons in MO; $\varepsilon_{HY}$ = Fermi level of redox electrons in the hydrogen reaction;$\varepsilon_M$ = Fermi level of the metal dissolution reaction.

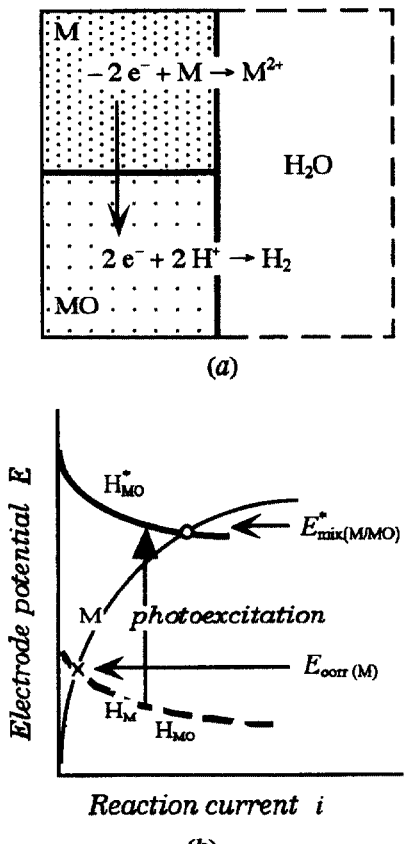


**Fig. 11.** Schemata for (a) local cell reactions and (b) their polarization curves at the M/$H_2O$ and MO/$H_2O$ interfaces on a photoexcited M-MO/$H_2O$ mixed electrode with a p-type semiconducting *MO* : M = anodic polarization curve of metal dissolution; $E_{HY}$ = equilibrium potential of the hydrogen reaction; $E_{corr}$ = corrosion potential of an isolated metal; $H^{*}_{MO}$ = cathodic polarization curve [Fermi level versus current] of the hydrogen evolution at the MO/$H_2O$ interface;$H_{MO}$ = cathodic invisible polarization curve [interfacial quasi-Fermi level of exited electrons versus current] of the hydrogen evolution at the MO/$H_2O$ interface;$H_M$ = cathodic polarization curve of the hydrogen evolution at the MO/$H_2O$ interface;$E_{mix}$ = mixed electrode potential of a photoexcited M-MO/$H_2O$ electrode.

### 3.7 Corrosion in oxygen-free environments

It follows from the foregoing that metals such as copper, which can not corrode in the absence of oxygen, may suffer under photoexcitation the corrosion involving hydrogen evolution when they are made contact with p-type oxide such as copper oxides even in oxygen-free environments.

It also follows that even in the environments where no oxygen is present, such as those under the deep ground, oxygen may possibly be produced on n-type oxides coupled with metals, if the oxides are exposed to the radiation of nuclear wastes.

## 4. Reduction-oxidation of surface oxides (electrochemical nature)

### 4.1 The redox potential of surface oxides

Surface oxides on metals may undergo reduction-oxidation reactions in which the valency of metallic ions changes such as shown in Eq.9:

$$MOH = MO + H^{+}_{aq} + e^{-} \qquad (9)$$

Iron rusts are known to be oxidized or reduced ferrous oxides and ferric oxides in aqueous solutions as represented by Eq.10:

$$3FeOOH + H^{+}_{aq} + e^{-} \leftrightharpoons Fe_3O_4 + 2H_2O \qquad (10)$$

Once the redox reaction is involved, the electrode

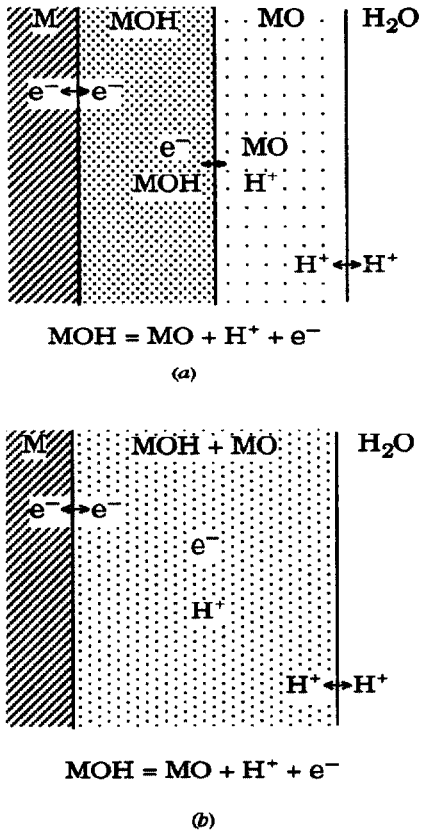


**Fig. 12.** Redox oxides MOH/MO in (a) two insoluble solid phase electrodes and (b) single soluble solid phase electrodes.

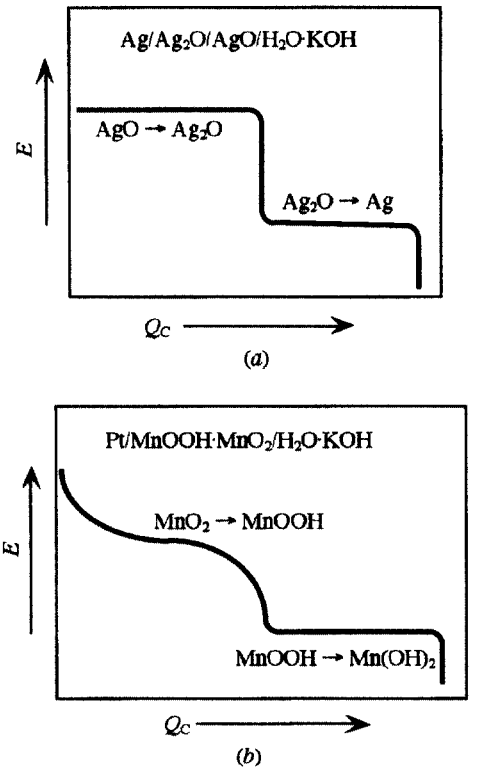


**Fig. 13.** Potential-charge curves of cathodic reduction of (a) two insoluble solid phase electrodes of AgO/$Ag_2O$ redox-oxides and (b) single soluble solid phase electrodes of $MnO_2$/MOOH redox-oxides.

potential of redox oxides is preferentially maintained somewhere around its equilibrium potential called the redox potential.

Two modes arise on redox-oxides; one is the two phase oxide electrode consisting of a higher and a lower valence oxide, and the other is the single phase electrode of a solid solution of the two oxides as shown in Fig. 12. In the former mode the charge transfer involves the transfer of electrons at the metal/lower oxide interface, the migration of electrons through the inner lower oxide layer, the redox reaction (the transfer of redox electrons and protons) at the lower oxide/higher oxide interface, and the transfer of protons through the outer layer and at the higher oxide/aqueous solution interfaces. The redox potential remains constant as long as the two oxides coexist as shown for AgO/$Ag_2O$ redox-oxides in Fig. 13(a). On the other mode of single phase oxides the redox potential depends on the concentration of lower and higher oxides, being lowered(more cathodic) with increasing concentration of the lower oxide as shown for $MnO_2$/MOOH redox-oxides in Fig. 13(b).

Note that the redox potential of redox-oxides is independent of the nature of the underlying metals, but is characteristic of the redox oxides themselves.

### 4.2 The mixed electrode potential of redox-oxides and corroding metals

The redox potential of oxides is usually higher (more anodic) than the corrosion potential of common metals. Surface redox-oxide thereby make the potential of corroding metals more anodic and hence tends to accelerate the corrosion.

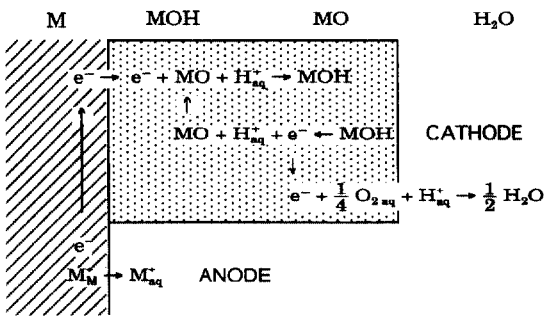


**Fig. 14.** Redox-oxides MOH/MO as an intermediate oxidant providing the cathodic reaction for metallic corrosion: The mixed electrode potential is maintained around the redox potential of the oxides which is usually more anodic than the corrosion potential of common metals.

Obviously, surface redox-oxide operate as oxidants on metallic corrosion in which the cathodic reduction of oxidized redox-oxides is coupled with the anodic dissolution. These surface redox-oxides in their reduced state may be oxidized by other oxidants such as gaseous oxygen whose redox potential is higher than that of redox-oxides. Fig. 14 shows a local corrosion cell in which a redox-oxide is involved as an intermediate oxidant in the cathodic reaction of local corrosion cell as illustrated in Eq. 10:

$$\frac{1}{4}O_{2aq} + H^{+}_{aq} + e^{-} \rightarrow \frac{1}{2}H_2O$$

cathodic reduction of oxygen (10a)

$$MOH \rightarrow MO + H^{+}_{aq} + e^{-}$$

anodic oxidation of redox-oxide (10b)

$$MO + H^{+}_{aq} + e^{-} \rightarrow MOH$$

cathodic reduction of redox-oxide (10c)

$$M_M \rightarrow M^{+}_{aq} + e^{-}$$

anodic metal dissolution (10d)

Since the reaction rate of hydrous redox-oxides is generally much greater than the rate of oxygen reduction on metals and oxides, the presence of redox-oxides increases the corrosion rate at potentials around the oxide redox potential as far as the oxidized state remains existing in the redox-oxides. The corrosion rate increased by the redox-oxides in the initial stage is then followed by its gradual decrease until it reaches a steady rate at which the oxygen reduction is balanced with the anodic metal dissolution when the oxidized state scarcely remains existing.

Received knowledge is that the presence of hydrous ferric oxides accelerates the corrosion of mild steels forming ferrous oxides in wet environment, while the ferrous oxide thus formed is oxidized to ferric oxides by atmospheric oxygen in relatively dry environment.

## 5. Summary

1) The rust layer of hydrous metal oxides is anion-selective in acidic solutions and cation-selective in basic solutions. The point of iso-selectivity, $pH_{pis}$, characteristic of individual metal hydroxides, is shifted toward acidic pH by the adsorption of multivalent oxoanions and toward basic pH by the adsorption of multivalent cations.

2) The anion-selecitive rust layer accelerates the localized corrosion by increasing the aggressive anion concentration in the occluded solution. The cation-selective rust layer inhibits the localized corrosion by removing aggressive hydrogen ions from the metal surface.

3) The anodically forward bipolar ion-selective rust layer, formed by the adsorption of multivalent oxoanions on an anion-selective rust layer, changes itself into a dehydrated oxide film accelerating the passivation of underlaying metals.

4) The oxide-covered metal electrode ($M/MO/H_2O$) presents itself as a semiconducting oxide electrode whose potential remains at the flat band potential of the oxide (MO), if no ionic transfer is involved in the electrode. The M-MO mixed electrode keeps its potential in between the corrosion potential of M and the flat band potential of MO.

5) The n-type surface oxide shifts the corrosion potential in the cathodic direction and reduces the metallic corrosion. Photoexcitation allows oxygen evolution to occur on the n-type oxide, which may be coupled with the cathodic oxygen reduction on the metal to form a photoexcited local cell of the oxidation-reduction of oxygen.

6) The p-type surface oxide shifts the corrosion potential in the anodic direction and increases the metallic corrosion. Photoexcitation allows the cathodic hydrogen evolution to occur on the p-type oxide, which may be coupled with the anodic metal dissolution to form a photoexcited local cell of the hydrogen evolution type of metallic corrosion even at electrode potentials more anodic than the hydrogen potential. Accordingly, metallic copper, which suffers no corrosion in the absence of oxygen, corrodes involving the cathodic hydrogen evolution on p-type copper oxides under photoexcitation even in oxygen-free environments.

7) The surface redox-oxide shifts the corrosion potential in the anodic direction and thus increases the metallic corrosion involving the cathodic reduction of the redox oxide.

## References


1. N. Sato, *Corrosion Science*, **37**, 1947 (1995).
2. W. J. Muller. "*Bedeckungstheorie der Passivitat der Metalle und ihre experimentalle Begrundung*", Verlag-Chemie, Berline,1933.
3. T. P. Hoar, in "*Modern Aspects of Electrochemistry*", Vol. **2**(Edited by J.O'M.Bockris), Butterworths, London, p.262 (1959).
4. N. Sato, *Electrochimica Acta*, **41**, 1525 (1996).
5. N. Sato, *Corrosion*, **45**, 354 (1989).
6. K. F. Bonhoeffer, *Z. Metallkunde*, **44**, 77 (1953), ;*Angew. Chem.*, **67**, 1 (1995).
7. N. Sato, *Corrosion Science*, **42**, 1957 (2000).
8. M. Sakashita and N. Sato, *Boshoku Gijutsu(Corrosion Engineering)*, **28**, 450 (1979).
9. M. Sakashita and N. Sato, *Corrosion*, **35**, 351 (1979).

10. K. Huber, *Z. Elektrochem.*, **59**, 693 (1953).
11. M. Suzuki, N. Masuko, and Y. Hisamatsu, *Boshoku Gijutsu*, **20**, 319 (1971).
12. M. Sakashita, Y. Yomura, and N. Sato, *Dennki Kagaku*, **45**, 165 (1977).
13. M. Sakashita and N.Sato, *Dennki Kagaku(J. Electrochem. Soc. Japan)*, **45**, 238 (1977).
14. M. Sakashita and N.Sato, *Corrosion Science*, **17**, 473 (1977).
15. Y. Yomura, M. Sakashita, and N.Sato, *Boshoku Gijutsu*, **28**, 64 (1979).
16. M. Sakashita and N.Sato, *Boshoku Gijutsu (Corrosion Engineering)*, **28**, 67 (1979).
17. M. Sakashita and N.Sato, *J. Electroanal. Chem.*, **62**, 127 (1975) .
18. M. Sakashita and N.Sato, *Dennki, Kagaku* **44**, 31 (1976).
19. M. Sakashita and N.Sato, *Dennki Kagaku*, **45**, 744 (1976).
20. M. Sakashita and N.Sato, *Boshoku Gijutsu (Corrosion Engineering)*, **25**, 3 (1976).
21. M. Sakashita, T. Shimakura, and N.Sato, *Proceedings. 9th International Congress on Metallic Corrosion*, Toronto, Canada, 3-7 June, 1984, National Research Council Canada, **1**, 126 (1984).
22. N.Sato, *Russian J. Electrochemistry*, **31**, 837 (1995).
23. J. Yuan and S. Tsujikawa, *J. Electrochem. Soc.*, **142**, 3444 (1995).
24. J. Yuan, R. Fujisawa, and S. Tsujikawa, *Zairyou-to-Kankyou (Material, and Environments, Japan)*, **43**, 433 (1994).
25. R. Fujisawa and S. Tsujikawa, *Materials Science Forum*, **183-189**, 1076 (1995).
26. N. Sato, "*Electrochemistry at Metal and Semiconductor Electrodes*", Elsevier, Amsterdam, The Netherland, p.325 (1998).